Composites Science and Technology 69 (2009) 2507–2513

Contents lists available at ScienceDirect

Composites Science and Technology

journal homepage: www.elsevier.com/locate/compscitech

# Antenna/sensor multifunctional composites for the wireless detection of damage

Ryosuke Matsuzaki [a,*], Mark Melnykowycz [b], Akira Todoroki [a]

[a] Department of Mechanical Sciences and Engineering, Tokyo Institute of Technology, 2-12-1 O-okayama, Meguro-ku, Tokyo 152-8552, Japan
[b] Rieter Automotive Management AG, Schlosstalstrasse 43, CH-8406 Winterthur, Switzerland

ARTICLE INFO

*Article history:*
Received 20 April 2009
Received in revised form 30 June 2009
Accepted 7 July 2009
Available online 30 July 2009

*Keywords:*
A. Functional composites
A. Smart materials
B. Electrical properties
D. Nondestructive testing
Wireless

ABSTRACT

Wireless structural health monitoring (SHM) techniques generally rely on the integration of sensors, transmitters, and antennas into structures; however, the ideal solution would entail the material itself acting as a monitoring system. The current work investigates the application of antenna/sensing multifunctional composites. In this technique, carbon fiber reinforced plastic (CFRP) structures are modeled as half-wavelength dipole antennas. The electrical or antenna property varies in accordance with damage occurrence and can be monitored wirelessly at a remote location. The feasibility of wireless SHM using the self-sensing antenna technique is investigated analytically and experimentally using unidirectional CFRP laminates and rotor blades of woven CFRP. The CFRP radiates radio energy well when it is used as a half-wavelength dipole antenna, and damages to the CFRP can be wirelessly detected by monitoring an increase in the resonant frequency of the CFRP antenna.



## 1. Introduction

Implementing an efficient integrated structural health monitoring (SHM) system into aircraft could prevent the occurrence of catastrophic failure during service by identifying damaged areas of a wing or fuselage and allowing time for repairs to be made. However, for the wired health monitoring of large-scale structures such as those used in the aerospace industry and civil engineering, it is often problematic that a large number of sensors need to be employed [1]. The large number of sensors requires complicated cabling and sophisticated acquisition instruments. The wireless monitoring of damage to in-service composite structures is highly sought after because it would enable low-cost performance and uncomplicated monitoring. In-service wired monitoring is especially difficult for rotating composite components such as helicopter blades, rotor shafts, and wind turbine blades. Moreover, wireless sensing is required for unmanned aerial vehicles (UAVs) since they are remotely controlled and monitored.

Regarding the wireless detection of damage to composites, a microelectromechanical system–interdigital transducer [2,3], a wireless sensor skin that is embedded in an inductor–capacitor resonant circuit [4], and remotely queried embedded microsensors [5] have been proposed. However, these use surface acoustic wave sensors or electromagnetic induction and the wireless range is thus normally short; for example, between rotor blades and a cockpit. Moreover, the structural and electrical components of engineering structures are generally considered to be separate, which increases the installation costs and weight.

In recent years, researchers have addressed the possibility of designing antennas that fulfill electrical as well as mechanical requirements and form the basis for composite antenna design. Conformal antenna arrays that are integrated into the composite skin of an aircraft have been proposed and demonstrated within the Smart-Skin Structure Technology Demonstration ($S^3$TD) program [6,7]. Popular solutions for the load-bearing antenna system are the conformal load-bearing antenna structure (CLAS) [8–11], the composite smart structure [12,13], and the surface antenna structure [14]. In a CLAS, a strip antenna is sandwiched between layers of Nomex honeycomb, which are then laminated with glass fiber reinforced plastic layers, resulting in a planar antenna structure that has a high bending stiffness and is conformal to shell surface designs such as aircraft wings or automobile roofs. The CLAS design, however, relies on traditional metallic materials for the electrically active radiating element. The surrounding Nomex and composite layers are essentially packaging materials, and the electrical and structural properties are not integrated. In addition to the problem of antenna integration, SHM techniques generally rely on embedding sensors into structures [2,3]; however, the ideal solution would entail the material itself acting as a monitoring system.

In previous studies [15,16], we used carbon fiber itself as a sensor in carbon fiber reinforced plastic (CFRP) for the wireless monitoring of applied strain, fiber breakage, and delamination. The method uses a voltage-controlled oscillator to convert the change in the electric resistance of the CFRP structures due to damage to changes in the oscillating frequency. The proposed method

* Corresponding author. Tel./fax: +81 3 5734 3184.
*E-mail address:* rmatsuza@ginza.mes.titech.ac.jp (R. Matsuzaki).

0266-3538/$ - see front matter © 2009 Elsevier Ltd. All rights reserved.
doi:10.1016/j.compscitech.2009.07.002

was applied to CFRP laminates, and oscillating frequencies at multiple locations were measured wirelessly in real time. However, many resistance–voltage converters and transmitting antennas are required to cover whole structures.

The present research realizes antenna/sensor multifunctional composites for the wireless detection of damage to CFRP structures. Using the high electrical conductivity of carbon fiber, the CFRP structures can be modeled as antennas and sensors in addition to having load-bearing capability. The electric properties of CFRP structures vary in accordance with damage such as fiber breakage or delamination; damage also affects the properties of the CFRP antenna. This change in the antenna property due to damage can be observed wirelessly at a remote location, and it provides information on the damage. Since CFRP acts as an antenna and sensor, a fully integrated load-bearing wireless SHM solution can be realized. In the present study, unidirectional CFRP and rotor blades made of woven composites are used as antenna materials. The feasibility of wireless SHM using the antenna/sensor multifunctional technique is investigated analytically and experimentally.

## 2. Antenna/sensor multifunctional composites

### *2.1. Concept*

There are a number of different antenna configurations that can be used for a CFRP antenna prototype. The most basic is a dipole antenna, which is traditionally made by suspending two wires with an insulator connecting their ends to one another. One end of the dipole has a current feed, and the opposite end is grounded. Since carbon fibers of CFRP have high electrical conductivity, a CFRP blade or wing structure may also act as a dipole antenna when electrical current is fed to the ends of the blade structures. The concept of a full antenna wing or blade structure is shown in Fig. 1. One end of the wing has a current feed, and the other end is grounded, producing the electrical field shown. The connecting points between two blades or wings must be electrically insulated. Since helicopter blades and UAV wings are usually assembled by mechanical joining, such insulation can be easily implemented and does not introduce any reduction in rigidity or strength. However, if both wings of an UAV were integrally molded and the carbon fibers are continuous in a longitudinal direction, the dipole model cannot be applied. In this case, a monopole antenna model will be applicable using a fuselage adopted as the electrical ground.

If there is serious damage such as fiber breakage, the antenna properties of the CFRP may change. The damage can then be detected wirelessly by evaluating the change in the antenna property. Moreover, by installing current feed cables to the ends of each wing, the whole area of the wings, which function as antennas, can be monitored. Since this method eliminates conventional structural cutouts, antenna joining, and sensor integration, and improves structural efficiency, most air vehicles could benefit from the proposed multifunctional composite technology.

### *2.2. Self-sensing using the change in the antenna property*

A half-wavelength dipole is a balanced antenna comprising two radiators that are each a quarter-wavelength. The voltage in the antenna element changes sinusoidally, and the feed point is at a voltage minimum and a current maximum. The voltage wavelength $\lambda$ is expressed as

$$\lambda = \frac{c}{f_0}, \tag{1}$$

where $f_0$ is the resonant frequency and $c$ is the speed of light, $3.0 \times 10^8$ m/s. The length of the half-wavelength dipole antenna $l$ corresponds to the half wavelength ($l = \lambda/2$). However, there is an imaginary part (reactance) associated with the input impedance of a dipole [17]. The reactance vanishes when the antenna length $l$ is equal to $\alpha\lambda/2$ where $\alpha$ is a length-shortening factor. Thus, the resonant frequency can be written using the antenna length $l$ as

$$f_0 = \alpha \frac{c}{2l}. \tag{2}$$

Usually the length of the dipole for the first resonance is about $l = 0.47$–$0.48\ \lambda$ depending on the radius of the wire. Note that even for the same element length, the resonant frequency can be adjusted; inductors connected to the antenna decrease the resonant frequency whereas capacitors increase the resonant frequency.

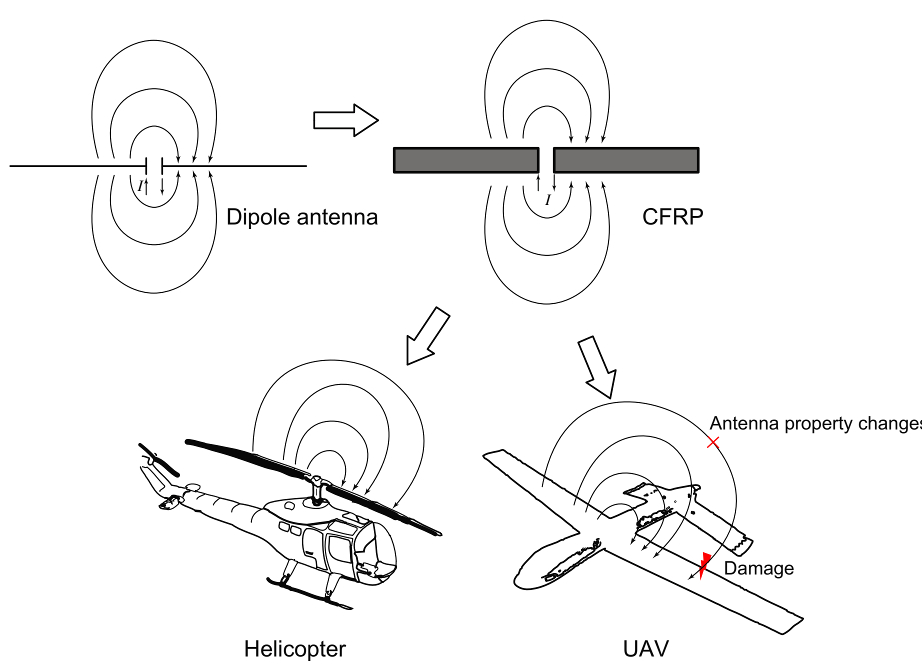


**Fig. 1.** Evolution of antenna configurations from a dipole to antenna/sensor multifunctional wing structures.

Since there are both reflected and incident waves, the antenna impedance $Z_L$ is expressed as [18]

$$Z_L = \frac{V_{inc} + V_{ref}}{I_{inc} + I_{ref}} = \frac{V_{inc} + V_{ref}}{\frac{V_{inc}}{Z_0} - \frac{V_{ref}}{Z_0}}, \quad (3)$$

where $V_{ref}$ is the reflected voltage, $V_{inc}$ is the incident voltage, $I_{inc}$ is the incident current, $I_{ref}$ is the reflected current, and $Z_0$ is the characteristic impedance of the line.

A signal traveling down a conductor reflects at the antenna length and a frequency mismatch occurs. The reflection coefficient $\Gamma$ is defined as the ratio of the reflected voltage to the incident voltage, and it is expressed using $Z_L$ and $Z_0$ from Eq. (3) as

$$\Gamma = \frac{V_{ref}}{V_{inc}} = \frac{Z_L - Z_0}{Z_L + Z_0}. \quad (4)$$

The reflection coefficient $\Gamma$ varies from −1 to +1, depending on the magnitude of the reflection. The return loss *RL* is the magnitude of the reflection coefficient in decibels and is expressed as

$$(RL)\,\mathrm{dB} = 20\log_{10}|\Gamma|. \quad (5)$$

If the antenna does not emit radio waves, the return loss *RL* is equal to zero, whereas if it perfectly emits radio waves, the return loss *RL* is negatively infinite. Since the return loss *RL* is a minimum at the resonant frequency, it is often used for resonant frequency estimation.

Next, let us consider the electric current applied to CFRP structures. Since CFRP is a conductive material, the structure may radiate radio waves and can be modeled as an antenna. Its resonant frequency $f_0$ depends on the length of the structure according to Eq. (2). When damage occurs within the structure and the electric current distribution in the CFRP changes, the antenna properties may also change; that is, since the damage interrupts the electric current path, as the modeled element length decreases, the corresponding resonant frequency increases.

From Eq. (2), the length of a damaged antenna element (or the damage location from the feeding point) can be approximately expressed as

$$l_x = \frac{\alpha c}{2f_0} - l_e, \quad (6)$$

where $l_x$ is the length of the damaged element while $l_e$ is the length of the other intact element. Thus, by measuring the resonant frequency shift from the intact state, the location of the damage can be estimated. When there is large damage penetrating the width, the electric current is interrupted and does not flow outward from that point. Thus, even if there are several damaged places, the damage closest to the feeding point is the critical one. On the other hand, if the damage is not so large and only a part of electric current is interrupted, the structure may act as a multiband antenna. In this case, the received power spectrum has multiple peaks corresponding to each antenna length.

Moreover, if the antenna impedance $Z_L$ in the intact state matches the line impedance $Z_0$, then $Z_L$ differs from $Z_0$ because of the damage, and return loss *RL* at the resonant frequency increases. This change in the antenna impedance $Z_L$ can also be estimated using return loss *RL* from Eqs. (4) and (5). Using the schematic diagram presented in Fig. 2, the relationship between the frequency and return loss *RL* tells us of damage occurrence and provides other information such as the location of the damage or the magnitude of the impedance change. In practical use, CFRP structures are used as transmitting antennas, and the power spectrum of radio waves received from such structures could be an indicator of structural health.

## 3. Antenna/sensor multifunctional composites using unidirectional CFRP laminates

### 3.1. Damaged antenna simulation

Using antenna simulation software, resonant frequencies are calculated for damage in one element. We used a full-wave, method-of-moments-based electromagnetic simulator, IE3D (Zeland Software, Inc.). The element model of a dipole antenna is 180 mm in length, 20 mm in width, and 1.6 mm in thickness. Each element is located at a distance of 5 mm, and the feeding points are located at the ends of the elements as shown in Fig. 3. Isotropic

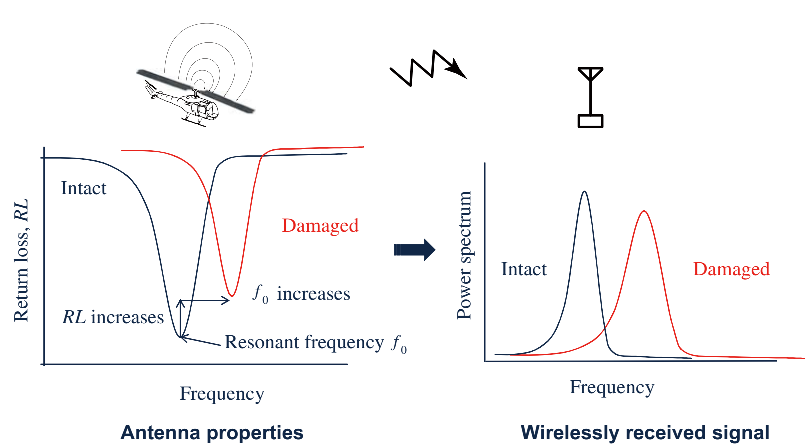


**Fig. 2.** Schematic diagram for antenna/sensor multifunctional composites that use changes in the antenna property.

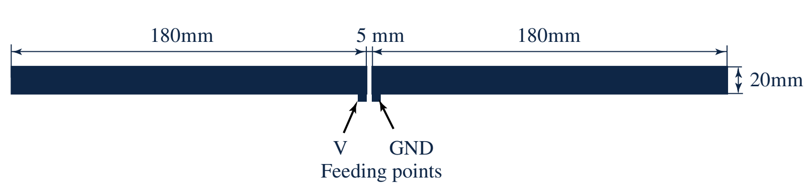


**Fig. 3.** Simulation model of a rectangular dipole antenna.

conductivity is used for simplicity. Note that electric current only flows in the longitudinal direction and not in the transverse direction, and electrical conductivity in the transverse direction does not greatly affect the antenna performance. The damaged antenna is modeled by shortening the element length, simulating that the electrical current is interrupted owing to fiber breakage.

Fig. 4 shows the return loss *RL* vs. frequency, with the length of one element shortened from 180 to 120, 80, and 20 mm to simulate antenna damage. The element length of 180 mm indicates the intact condition, while a shortened element length indicates fiber breakage at that distance from the feed point. In case that the elements are intact, the return loss *RL* has a minimum at the resonant frequency of about 390 MHz, which agrees with the frequency calculated using Eq. (2) considering $\alpha = 0.94$. As the element is shortened, the resonant frequency increases as shown in Fig. 4. In addition, an increase in the return loss, or a decrease in the dip magnitude, is also observed. This indicates that the antenna radiation ability decreases because the antenna is not an ideal half-wavelength dipole antenna.

From this simulation, we can estimate damage occurrence by detecting a shift in the resonant frequency or magnitude of the return loss. Moreover, from the shift in the resonant frequency, we can estimate the length of the damaged element by referring to the simulation results as shown in Fig. 4. The changes in the return loss property also lead to peak shift or reduction of the power spectrum of the signal wirelessly received from the CFRP antenna structure. However, the magnitude of the peak of the power spectrum is also affected by conditions of the wireless transmission environment such as the wireless range, output power, and weather conditions. For example, as the wireless range becomes longer, the power of the received signal reduces in amplitude. Microwaves also suffer severe attenuation because of water vapor in the atmosphere. These conditions decrease the power spectrum of received radio waves. Thus, the resonance frequency shift should be used for the detection of damage and estimation of its location. Here, the frequency of the dynamic vibration of structures is usually up to a few kHz, and much lower than that of an alternating current, of just several hundred MHz. Therefore, even if some electrical noise caused by structural vibration occurs, it does not affect the power spectrum in the high frequency range.

### 3.2. Experimental procedures

Laminated CFRP rectangular specimens are fabricated using Pyrofil 380, a carbon/epoxy prepreg produced by Mitsubishi Rayon

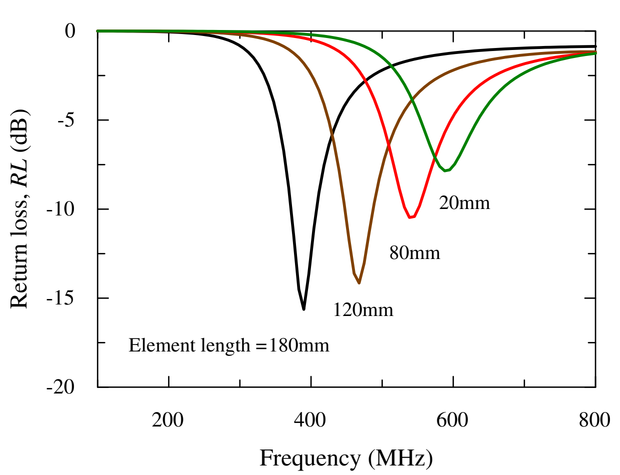


**Fig. 4.** Simulated frequency response of the return loss *RL* to changes in the element length.

Co. Ltd. The stacking sequence of the laminates is $[0_7]_T$, where zero degrees indicates the longitudinal direction. The curing temperature is 130 °C, the curing time 90 min, and the curing pressure 0.7 MPa. The specimen is 180 mm in length, 20 mm in width, and 1.6 mm in thickness, as for the simulation model shown in Fig. 3. To feed the electric current, electrodes are mounted on the specimen surface 5 mm from the specimen edge. The electrodes are fabricated with a silver paste after polishing the surface of the specimen with abrasive paper to remove extra resin and so obtain a good electric contact between the silver paste and carbon fibers. The electrodes are then covered with epoxy resin for protection.

To investigate the antenna properties of CFRP specimens, the antenna return loss *RL* is measured using a return loss bridge (Kuranishi Instruments, BR-1), spectrum analyzer (Advantest, TR4131), and signal generator (Anritsu, MG3602A) as shown in Fig. 5. The frequency of the sinusoidal wave from the signal generator is swept in the target frequency range, and the power spectrum is recorded with the spectrum analyzer at each frequency.

Next, wireless measurement tests are conducted. The CFRP specimen is used for the transmitting dipole antenna and an aluminum dipole antenna is used for the receiving antenna. The experimental setup is shown in Fig. 6. The wireless distance is set to 1 m. The signal generator sweeps the target frequency range, the radio waves transmitted from the CFRP antenna are received at the aluminum dipole antenna, and the power spectrum is observed using the spectrum analyzer.

Damage was introduced 80 mm from the outer edge of the specimen (element length 100 mm) by three-point bending. Fig. 7 shows the damaged specimen. The damage includes delamination and fiber breakage in the surface layer. Although researchers have shown that electrical properties change with less severe damage such as applied strain, matrix cracking, and delamination [19], the pilot test in this research targets more severe damage that includes fiber breakage, which leads to enormous changes in electrical resistance.

### 3.3. Results and discussion

Fig. 8 shows the two-dimensional antenna radiation pattern using the CFRP rectangular specimen as half-wavelength dipole elements. The analytical value was obtained by antenna simulation using MMANA software, which is based on numerical electromagnetics code [17]. The experimental radiation pattern agrees well with the simulation results; hence, it is confirmed that the CFRP rectangular structure functions well as a dipole antenna.

Fig. 9 shows the frequency response of the antenna return loss *RL* using the CFRP rectangular specimen as a dipole antenna. The abscissa is the swept frequency and the ordinate is the return loss *RL*. Since the antenna radiates maximum radio energy at the resonant frequency, the return loss *RL* has a minimum at that frequency. It is seen from the experimental results that the intact CFRP specimen has a resonant frequency of 330 MHz while the analytical resonant frequency is about 390 MHz as shown in Fig. 4. The discrepancy may be due to an inductance effect around the electrodes, the CFRP itself, or electromagnetic effects around the antenna.

Fig. 9 also shows the frequency response of return loss *RL* of the damaged specimen. The resonant frequency increases to 570 MHz as the antenna element length shortens owing to interruption of the electric current path. The analytical resonant frequency obtained using the IE3D software is also shown in Fig. 9, and the trend of the increase in frequency due to damage agrees with the experiments. There is frequency discrepancy, as observed for the intact specimen. The return loss *RL* at the resonant frequency increases owing to damage because the antenna impedance and

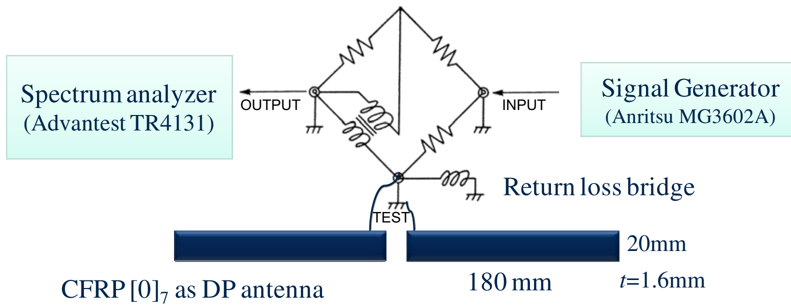


**Fig. 5.** Experimental setup for return loss measurements of CFRP dipole antennas.

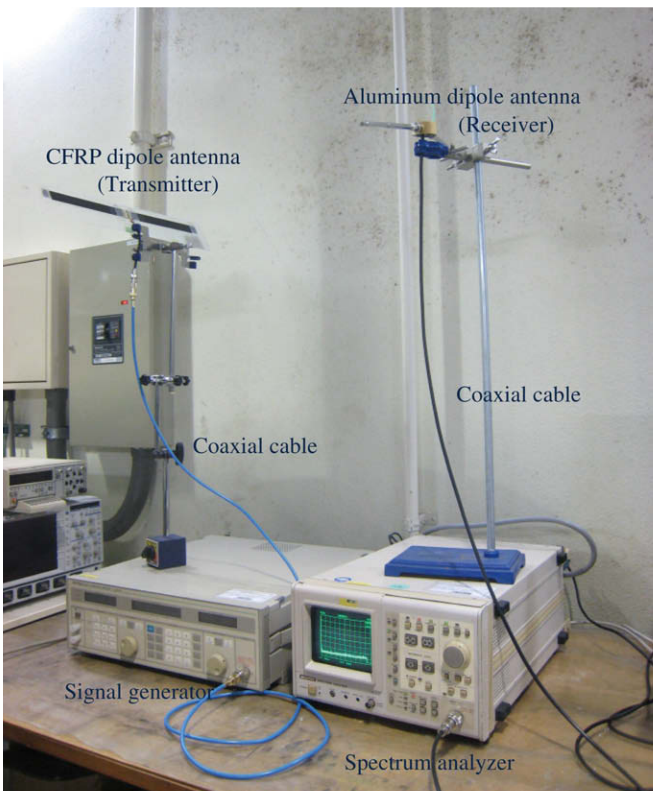


**Fig. 6.** Experimental setup for wireless damage detection tests. CFRP is used for the transmitting antenna while an aluminum dipole is used as the receiving antenna. The distance between the two antennas is set to 1 m in the experiments.

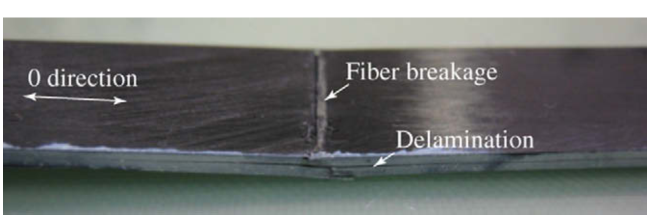


**Fig. 7.** Damaged CFRP rectangular specimen after three-point bending.

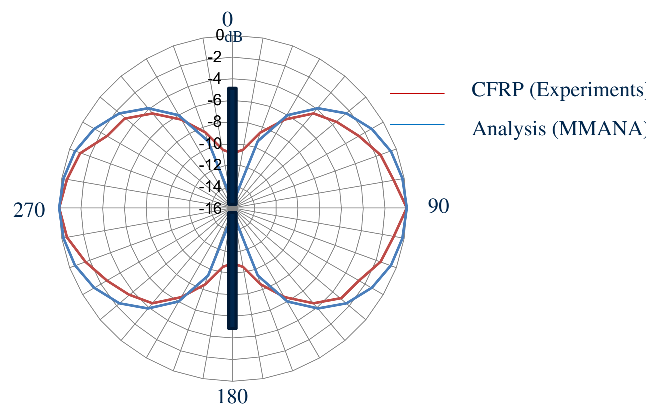


**Fig. 8.** Experimental and analytical two-dimensional radiation patterns of dipole antennas using the CFRP rectangular specimens. The analytical pattern was obtained using the antenna simulation software MMANA.

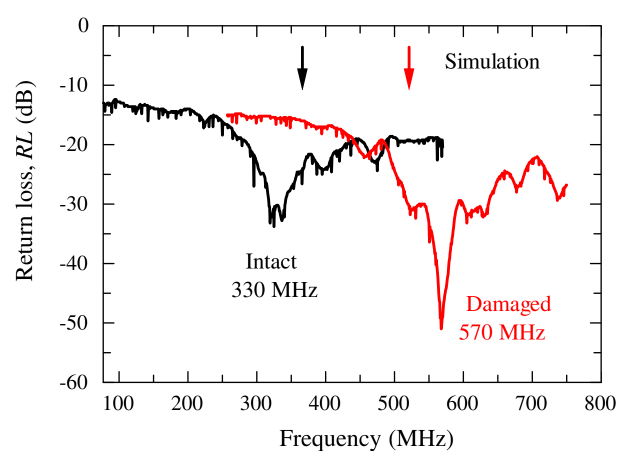


**Fig. 9.** Frequency response of the return loss *RL* of intact and damaged CFRP rectangular specimens as antennas. The arrows indicate the simulated resonant frequencies obtained using the IE3D simulator.

characteristic impedance of the line were not matched precisely in this test. If the impedance of the intact antenna is lower than the characteristic impedance, the damaged antenna impedance becomes higher and closer to the characteristic impedance, resulting in a reduction of the impedance mismatch.

Fig. 10 shows the power spectrum of radio waves wirelessly received from the CFRP dipole antenna by sweeping frequency. The power spectrum peaks at 330 MHz and 570 MHz for the intact and damaged specimens, respectively. These frequencies agree well with the results of the return loss experiments though there is some radio noise observed in the wireless tests.

These results confirm that a damaged specimen can be modeled as a shortened antenna element and that its resonance frequency is increased by the damage. Thus the feasibility of wireless SHM using CFRP rectangular structures as antennas was demonstrated. Moreover, by measuring the frequency shift from the frequency for the intact specimen, the approximate location of the damage

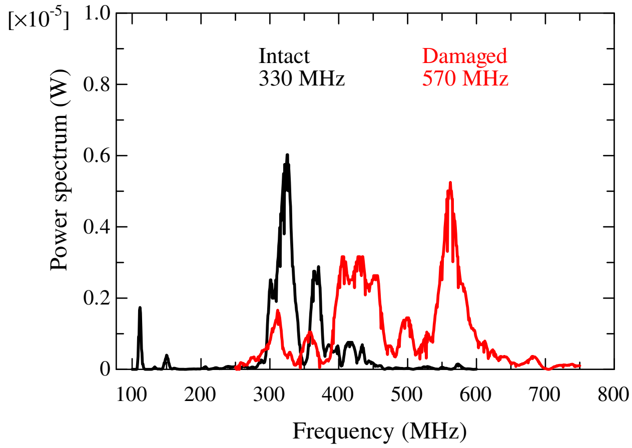


**Fig. 10.** Power spectrum of a wirelessly received signal from intact and damaged CFRP rectangular specimens as antennas.

can be estimated. To validate this effectiveness more precisely, further experiments in which the location of damage is changed will be carried out in the future.

## 4. Application to rotor blades of woven CFRP

### 4.1. Experimental procedures

The proposed antenna/sensor multifunctional technique was applied to rotor blades (E-sky, EK4-0012). Each blade is a cored sandwich structure; the material of the blade skin is woven CFRP $[0/90]_T$ and the core is filled with urethane foam. The length is 335 mm, the width is 32 mm, and the thickness is 4.5 mm. The surface of the inner edge of the blade is abraded and electrodes are fabricated with copper film adhered using silver paste as shown in Fig. 11. Similar to the tests using the rectangular CFRP specimens, antenna return loss and wireless tests are conducted. Severe damage including fiber breakage is introduced 120 mm from the outer edge as shown in Fig. 12 by three-point bending.

### 4.2. Results and discussion

Fig. 13 shows the frequency response of the return loss *RL* of the rotor blade used as a half-wavelength dipole antenna. The abscissa is the swept frequency and the ordinate is the return loss *RL*. The intact state has a resonant frequency of 180 MHz. The calculated

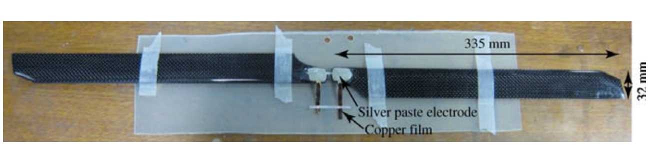


**Fig. 11.** Woven composite rotor blades for antenna/sensor multifunctional composites.

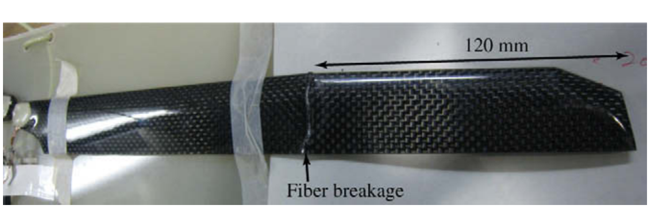


**Fig. 12.** Damaged blades after three-point bending.

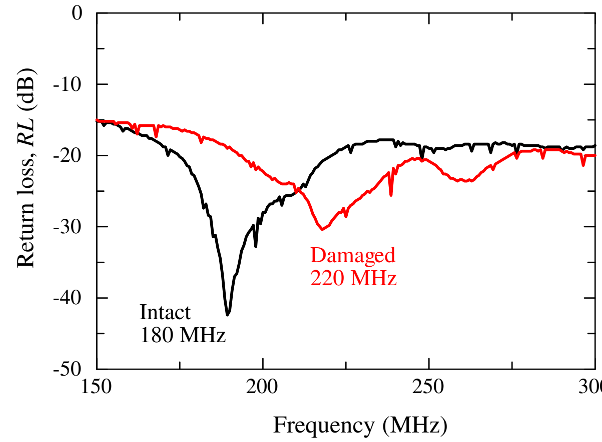


**Fig. 13.** Frequency response of the return loss *RL* for CFRP rotor blades as antennas.

resonant frequency from Eq. (2) for $\alpha = 0.8$ is about 179 MHz. In the damaged condition, the resonant frequency shifts to a higher frequency of 220 MHz.

In the wireless tests, the CFRP rotor blade modeled as a dipole antenna transmitted radio waves to an aluminum dipole antenna. Fig. 14 shows the power spectrum of the signal wirelessly received at the aluminum dipole antenna. The abscissa is the swept frequency and the ordinate is the power spectrum of the received signal. The power spectrum peak shifts to a higher frequency because of the damage, and this frequency shift agrees well with the results of the return loss experiments as shown in Fig. 13. Thereby, by measuring the frequency shift of the power spectrum peak, the damage can be detected wirelessly without installation of any antenna or sensor. These results clearly demonstrate the feasibility of antenna/sensor multifunctional composites for CFRP rotor blades.

Fig. 15 shows an estimation of damage location using Eq. (6) and the obtained resonant frequencies. The abscissa is the actual damage location from the feeding point, and the ordinate is the estimated damage location. Solid circles indicate estimated results from the simulation in Fig. 4, while the open triangle symbols show the experimental results of unidirectional CFRP and CFRP blades. It was confirmed that the approximate location of the damage can be estimated by measuring the resonant frequency change. The slight estimation error in unidirectional CFRP may be caused by the inductance effect, as mentioned in Section 3.3.

In its current form, the use of CFRP for antenna-based SHM has proven useful for the detection of catastrophic events. A UAV could

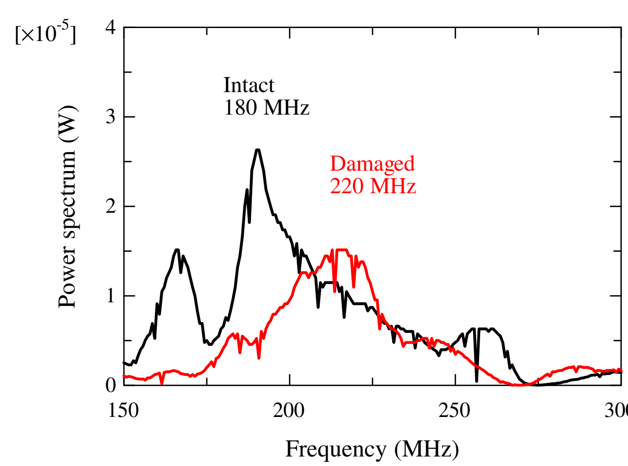


**Fig. 14.** Power spectrum of the wireless signal transmitted from CFRP rotor blades as antennas. The frequency of the transmitter is swept from 150 to 300 MHz.

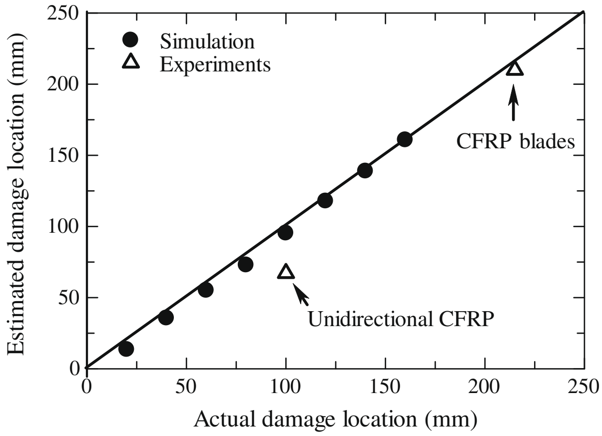


**Fig. 15.** Estimated damage location using the resonant frequency of received radio waves.

benefit from such SHM technology. In principle, a UAV flies according to set flight parameters. If a UAV is damaged from anti-aircraft fire that destroys part of the wing, this would be automatically known and the UAV could implement new flight controls based on the known length of the wing structure, which would be determined using the antenna SHM technique.

## 5. Conclusions

The current work has shown that CFRP can be used as an antenna/sensor material. This technique enables the wireless SHM of whole CFRP structures functioning as an antenna, which reduces the number of sensors and amount of wireless equipment required. Comparing with the analytical antenna radiation pattern, we confirmed that CFRP rectangular laminates radiate radio energy well when used as half-wavelength dipole antennas. The feasibility of wireless SHM using the proposed multifunctional composites was investigated using unidirectional CFRP laminates and rotor blades of woven CFRP. The experiments demonstrated that the damaged specimen can be modeled as shortened antenna elements and that its resonance frequency is increased by the damage. It was also confirmed from antenna simulation and experimental results that the approximate location of the damage can be estimated by measuring the frequency shift from the frequency of the intact specimen.

## References

[1] Los Alamos National Laboratory. A review of structural health monitoring literature: 1996–2001. LA-13976-MS; 2003.
[2] Varadan VK. Wireless microsensors for health monitoring of aircraft structures. In: Proceedings of SPIE; 2003. p. 175–88.
[3] Varadan VK, Varadan VV. Design and development of smart skin conformal antenna with MEMS structural sensors and actuators. In: Proceedings of SPIE; 1997. p. 94–105.
[4] Carlson JA, English JM, Coe DJ. A flexible, self-healing sensor skin. Smart Mater Struct 2006;15(5):N129–35.
[5] Krantz DG, Belk JH. Remotely-queried wireless embedded microsensors in composites. In: Proceedings of SPIE; 1997. p. 219–26.
[6] Lockyer AJ, Alt KH, Kinslow RW, Kan H-P, Kudva JN, Tuss J. Development of a structurally integrated conformal load-bearing multifunction antenna: overview of the air force smart skin structures technology demonstration program. In: Proceedings of SPIE; 1996. p. 55–64.
[7] Lockyer AJ, Alt KH, Coughlin DP, Durham MD, Kudva JN, Goetz AC. Design and development of a conformal load-bearing smart-skin antenna: overview of the AFRL smart skin structures technology demonstration (S3TD). In: Proceedings of SPIE; 1999. p. 410–24.
[8] Jeon JH, Hwang W, Park HC, Park WS. Buckling characteristics of smart skin structures. Compos Struct 2004;63(3–4):427–37.
[9] Jeon JH, You CS, Kim CK, Hwang W, Park HC, Park WS. Design of microstrip antennas with composite laminates considering their structural rigidity. Mech Compos Mater 2002;38(5):447–60.
[10] Lockyer AJ, Alt KH, Kudva JN, Kinslow RW, Goetz AC. Structural finite-element modeling strategies for conformal load-bearing antenna structure (CLAS) (Air Force Contract F33615-C-93-3200). In: Proceedings of SPIE; 1997. p. 166–72.
[11] Yao L, Qiu Y. Design and fabrication of microstrip antennas integrated in three dimensional orthogonal woven composites. Compos Sci Technol; 2009;69(7–8):1004-8.
[12] You CS, Hwang WB. Design of load-bearing antenna structures by embedding technology of microstrip antenna in composite sandwich structure. Compos Struct 2005;71(3–4):378–82.
[13] You CS, Hwang WB. Antenna integration with composite sandwich structures using gain enhancement methods. J Compos Mater 2007;41(9):1037–49.
[14] Kim DH, Hwang W, Park HC, Park WS. Fatigue characteristics of a surface antenna structure designed for satellite communication. J Reinf Plast Compos 2005;24(1):35–51.
[15] Matsuzaki R, Todoroki A. Wireless detection of internal delamination cracks in CFRP laminates using oscillating frequency changes. Compos Sci Technol 2005;66:407–16.
[16] Matsuzaki R, Todoroki A, Takahashi K. Time-synchronized wireless strain and damage measurements at multiple locations in CFRP laminate using oscillating frequency changes and spectral analysis. Smart Mater Struct 2008;17(5):1–9.
[17] Balanis CA. Antenna theory: analysis and design. 3rd ed. Wiley-Interscience; 2005.
[18] Carr JJ. Practical antenna handbook. McGraw-Hill; 2001.
[19] Todoroki A, Ueda M, Hirano Y. Strain and damage monitoring of CFRP laminates by means of electrical resistance measurement. J Solid Mech Mater Eng 2007;1(8):947–74.